

# HIGH-QUALITY LINEAR INTERPOLATION FOR DEMOSAICING OF BAYER-PATTERNED COLOR IMAGES

*Henrique S. Malvar, Li-wei He, and Ross Cutler*

Microsoft Research  
One Microsoft Way, Redmond, WA 98052, USA

## ABSTRACT

This paper introduces a new interpolation technique for demosaicing of color images produced by single-CCD digital cameras. We show that the proposed simple linear filter can lead to an improvement in PSNR of over 5.5 dB when compared to bilinear demosaicing, and about 0.7 dB improvement in R and B interpolation when compared to a recently introduced linear interpolator. The proposed filter also outperforms most nonlinear demosaicing algorithms, without the artifacts due to nonlinear processing, and a much reduced computational complexity.

## 1. INTRODUCTION

Digital cameras are quite popular today; many users are switching away from regular film photography. For cost reduction, most digital cameras use a single charge-coupled device (CCD) sensor, with the CCD pixels preceded in the optical path by a color filter array (CFA) in a Bayer mosaic pattern, as shown in Fig. 1. For each  $2 \times 2$  set of pixels, two diagonally opposed pixels have green filters, and the other two have red and blue filters. Since G carries most of the luminance information for humans, its sampling rate is twice that of R and B.

We call demosaicing the problem of interpolating back the image captured with a CFA, so that for every CCD pixel we can associate a full RGB value. The simplest approach to demosaicing is bilinear interpolation [1]–[4], in which the three color planes are independently interpolated using symmetric bilinear interpolation from the nearest neighbors of the same color. As expected, bilinear interpolation generates significant artifacts, especially across edges and other high-frequency content, since it doesn't take into account the correlation among the RGB values. Practical demosaicing algorithms take such correlation into ac-

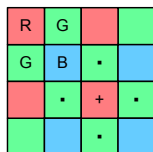


**Figure 1.** Typical Bayer mosaic for color image capture in single-CCD digital cameras; the G subimage has twice as many pixels as the R and B subimages.

count, either with better linear filters [4], or with nonlinear filters that adapt interpolation smoothness to a measure of image activity or edginess [1]–[4].

In this paper we present a simple linear demosaicing filter, with better performance and lower complexity than that in [4]. Our filter also outperforms many nonlinear algorithms. In Section 2 we quickly review some of the techniques proposed for improved demosaicing performance, and in Section 3 we present our new linear filter. Performance comparisons and conclusions are presented in Sections 4 and 5, respectively.

## 2. BEYOND BILINEAR DEMOSAICING

Referring to Fig. 1, in bilinear demosaicing the green value  $g(i,j)$  at a pixel position  $(i,j)$  that falls in a red or blue pixel, is computed by the average of the neighboring green values in a cross pattern:

$$\hat{g}(i,j) = \frac{1}{4} \sum_{(m,n) \in \{(0,-1), (0,1), (-1,0), (1,0)\}} g(i+m, j+n) \quad (1)$$

which corresponds to estimating the green value at the pixel marked ‘+’ in Fig. 1 as the average of the observed green values marked ‘.’. At image boundaries, only pixels that fall within the image are included, and the scaling adjusted. For the R and B colors the same equation applies (with a diagonal cross pattern), except that for pixel positions  $(i,j)$  that fall in a green pixel only two red neighboring values are averaged to produce an interpolated red value; the same holds for blue. Besides the computational simplicity of (1), its output value is guaranteed to have the same dynamic range of the input value, so no overflow logic is needed on the output value.

Exploiting the correlation among the RGB channels is the main idea for improving demosaicing performance. Specifically, we can assume that in a luminance/chrominance decomposition, the chrominance components don't vary much across pixels. In the constant-hue approach of Freeman [2],[5], the green channel is bilinearly interpolated, and then the R and B channels are interpolated such as to maintain a constant hue, defined as the R/G and B/G ratios. Even at the expense of computing those divisions, it still produces visible artifacts [2]. Better results can be obtained by starting with bilinearly interpolated G pixels, and

applying median filters to the interpolated values of the color differences R – G and B – G [2].

Improved performance can be obtained with gradient-based methods [2],[6], which typically estimate edge directions and adjust the interpolation formulas so that filtering is performed preferentially along edge directions, and not across them. For example, for interpolating the green channel in Laroche and Prescott’s method, the R and B channels are used to determine edge directions, which determine unequal weights to the terms in (1) for the green channel; the color differences R–G and B–G are then interpolated [2],[6]. Hamilton and Adams’ method improves on Laroche and Prescott’s by considering both first- and second-order pixel differences [6],[7]. Chang, Cheung, and Pang improved on that by considering a variable number of gradients [8]. A simpler but efficient algorithm that uses soft decision rules to combine interpolation results from horizontal and vertical directions is presented in [9].

Iterative methods can lead to further improvement by using results from B and R interpolation to correct the G interpolation, and vice-versa. That is the basis of Kimmel’s approach 0, where the interpolation steps are based on a combination of the constant-hue and gradient-based methods. A technique based on iterative projections is presented in [6]. It has the best performance to date on a popular set of standard test images, but it has a very high complexity (as many as 480 operations per input pixel). So, the method in [6] can be seen as setting performance bounds to what can be achieved with more practical algorithms.

### 3. IMPROVED LINEAR INTERPOLATION

It is interesting to note that most of the algorithms discussed in the previous section use nonlinear filters whose region of support go beyond immediately adjacent pixels. That raises a simple question, which was not addressed in [1]–[9]: what is the best performance we can get from a linear filter whose region of supports extends to, say, a 5×5 pixel region?

Pei and Tam proposed a good solution along those lines [4], by first estimating R and G via bilinear interpolation, then estimating the color differences B – G and R – G from those, smoothing the color differences via 4-point averages (under the assumption that the color differences are slowly-varying), and finally using those to interpolate the G values and then to do a final estimate of the R and B values. Their unrolled interpolation equations are equivalent to linear filters operating on a 5x5 pixel window around the current pixel [4].

#### 3.1 The Proposed Interpolation Method

Instead of using a constant or near-constant hue approach like the methods described above, we propose the use of the following criterion: edges have much stronger luminance than chrominance components. Thus, when we look at interpolation of a green value at a red pixel location, for example, we don’t discard the red value at that location – it is valuable information! Rather, we compare that red value to its estimate for a bilinear interpolation for the nearest red samples. If it is different from that estimate, it probably means there’s a sharp luminance change at that pixel,

and thus we correct a bilinearly interpolated green value by adding a portion of this estimated luminance change.

Specifically, to interpolate G values at an R location, for example (the ‘+’ pixel in Fig. 1), we use the formula

$$\hat{g}(i, j) = \hat{g}_B(i, j) + \alpha \Delta_R(i, j) \quad (2)$$

where  $\Delta_R(i, j)$  is the gradient of R at that location, computed by

$$\Delta_R(i, j) \triangleq r(i, j) - \frac{1}{4} \sum_{(m, n) \in \{(0, -2), (0, 2), (-2, 0), (2, 0)\}} r(i + m, j + n) \quad (3)$$

The subscript *B* in (2) means bilinearly interpolated, as in (1). So, we correct the bilinear interpolation estimate by a measure of the gradient  $\Delta_R$  for the known color at the pixel location, which is estimated by the simple formula in (3). The gain factor  $\alpha$  controls the intensity of such correction.

Thus, our method is in fact a gradient-corrected bilinear interpolated approach, with a gain parameter to control how much correction is applied. For interpolating G at blue pixels, the same formula is used, but corrected by  $\Delta_B(i, j)$ . For interpolating R at green pixels, we use the formula

$$\hat{r}(i, j) = \hat{r}_B(i, j) + \beta \Delta_G(i, j) \quad (4)$$

with  $\Delta_G(i, j)$  determined by a 9-point region, as shown in Fig. 2. For interpolating R at blue pixels, we use the formula

$$\hat{r}(i, j) = \hat{r}_B(i, j) + \gamma \Delta_B(i, j) \quad (5)$$

with  $\Delta_B(i, j)$  computed on a 5-point region, also shown in Fig. 2. The formulas for interpolating B are similar, by symmetry.

#### 3.2 Gradient-Correction Gains

To determine appropriate values for the gain parameters  $\{\alpha, \beta, \gamma\}$ , we used a Wiener approach; that is, we computed the values that led to minimum mean-square error interpolation, given second-order statistics computed from a good data set (the Kodak image set used in [6]). We then approximated the optimal Wiener coefficients by integer multiples of small powers of 1/2, with the final result  $\alpha = 1/2$ ,  $\beta = 5/8$ , and  $\gamma = 3/4$ . From the values of  $\{\alpha, \beta, \gamma\}$  we can compute the equivalent linear FIR filter coefficients for each interpolation case. The resulting coefficient values, shown in Fig.2, make the filters quite close (within 5% in terms of mean-square error) to the optimal Wiener filters for a 5×5 region of support.

Thus, we believe that the only way to design a practical linear filter with a lower mean-square interpolation error would be to use larger regions of support. That would not only increase computational complexity and memory footprint, but it would also lead to ringing artifacts around edges.

One way to evaluate computational complexity is to count the number of nonzero filter coefficients within the 5×5 regions of support. For Pei-Tam’s method [4], there are 9 nonzero coefficients for the G channel, and an average of 13 each for the R and B channels. Our method has a slightly lower complexity: 9 coefficients for the G channel and 11 each for R and B.

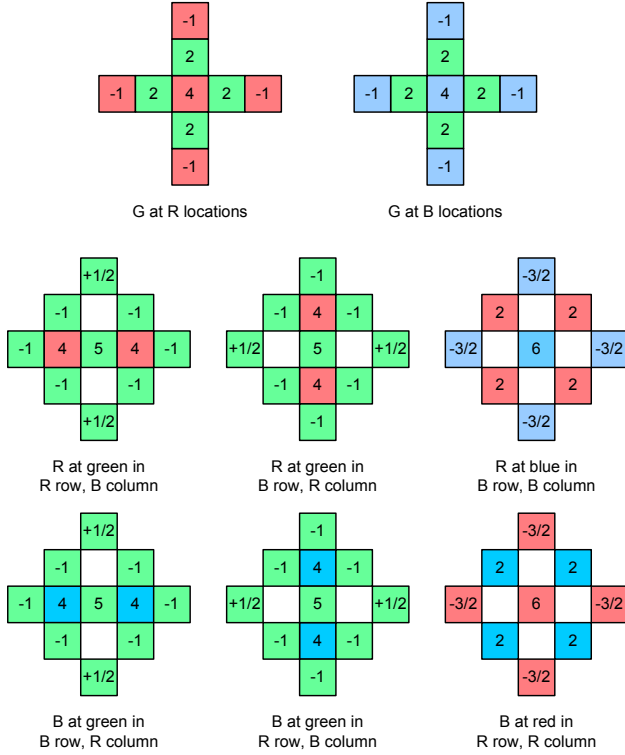


Figure 2. Filter coefficients for our proposed linear

#### 4. PERFORMANCE

We compared our proposed method to several others, using the Kodak image set [6], by simulating a Bayer sampling array (simply by keeping only one of each of the RGB values for each pixel, as in Fig. 1) and then applying the various interpolation algorithms. This subsampling approach is not really representative of digital cameras, which usually employ careful lens design to effectively perform a small amount of lowpass filtering to reduce the aliasing due to the Bayer pattern subsampling. However, since all papers in the references perform just subsampling, with no lowpass filtering, we did the same so we could compare results. We have also tested all interpolation methods with small amounts of Gaussian lowpass filtering before Bayer subsampling, and found that the relative performances of the methods are roughly the same, with or without filtering. The improvement in peak-signal-to-noise ratio (PSNR) over bilinear interpolation is shown in Table 1. Except for Freeman’s method, most approaches lead to more than 5 dB improvement, and our proposed method on average outperforms all others.

Besides PSNR measurements, we need to verify visual quality. Fig. 3 shows the interpolated results for one of the images in the Kodak set. From those we see that our proposed method leads to a quality similar to a good nonlinear method such as Kimmel’s 0, but with a much lower complexity. Compared to Pei-Tam linear filters, our method produces slightly less visible color fringing distortion, as well as a lower PSNR, at a slightly reduced computational complexity.

| #           | ch | A           | B           | C           | D           | E           | F           |
|-------------|----|-------------|-------------|-------------|-------------|-------------|-------------|
| 1           | R  | 3.44        | 5.58        | 4.17        | 8.17        | 4.74        | 5.56        |
|             | G  | 0.00        | 5.26        | 6.62        | 5.55        | 6.09        | 6.09        |
|             | B  | 3.74        | 5.82        | 3.94        | 8.05        | 5.28        | 5.87        |
| 2           | R  | 2.46        | 3.99        | 3.68        | -1.52       | 4.05        | 4.34        |
|             | G  | 0.00        | 4.60        | 5.10        | 2.20        | 4.76        | 4.76        |
|             | B  | 3.34        | 5.04        | 4.66        | 4.75        | 4.67        | 4.48        |
| 3           | R  | 3.80        | 6.05        | 6.56        | 4.67        | 5.68        | 6.84        |
|             | G  | 0.00        | 6.66        | 6.27        | 0.12        | 7.52        | 7.52        |
|             | B  | 3.76        | 5.98        | 6.14        | 7.17        | 5.34        | 6.50        |
| 4           | R  | 3.48        | 5.80        | 4.47        | 8.22        | 5.16        | 5.81        |
|             | G  | 0.00        | 5.20        | 6.19        | 5.02        | 5.92        | 5.92        |
|             | B  | 3.38        | 5.50        | 4.42        | 6.63        | 4.18        | 4.97        |
| 5           | R  | 3.89        | 5.67        | 5.99        | 4.61        | 4.82        | 6.20        |
|             | G  | 0.00        | 5.79        | 5.67        | -3.01       | 5.71        | 5.71        |
|             | B  | 3.65        | 5.44        | 6.05        | 5.04        | 4.67        | 5.81        |
| 6           | R  | 3.49        | 6.29        | 3.42        | 9.50        | 5.22        | 5.68        |
|             | G  | 0.00        | 6.16        | 6.63        | 6.41        | 5.72        | 5.72        |
|             | B  | 3.50        | 6.27        | 3.33        | 9.12        | 4.99        | 5.52        |
| 7           | R  | 3.70        | 6.00        | 5.09        | 7.97        | 4.75        | 5.75        |
|             | G  | 0.00        | 5.95        | 6.14        | 3.75        | 5.90        | 5.90        |
|             | B  | 3.48        | 5.86        | 4.71        | 7.75        | 4.29        | 5.38        |
| 8           | R  | 3.68        | 5.92        | 5.71        | 7.41        | 5.19        | 6.29        |
|             | G  | 0.00        | 6.19        | 6.83        | 6.23        | 6.86        | 6.86        |
|             | B  | 3.46        | 5.65        | 5.56        | 8.08        | 4.87        | 5.92        |
| 9           | R  | 3.40        | 5.30        | 5.01        | 6.22        | 5.04        | 5.68        |
|             | G  | 0.00        | 5.00        | 5.83        | 2.30        | 5.84        | 5.84        |
|             | B  | 3.64        | 5.45        | 5.15        | 6.54        | 4.83        | 5.47        |
| 10          | R  | 3.33        | 5.75        | 4.48        | 7.57        | 4.07        | 4.91        |
|             | G  | 0.00        | 6.10        | 6.44        | 5.91        | 5.64        | 5.64        |
|             | B  | 3.46        | 5.98        | 4.53        | 7.82        | 4.61        | 5.31        |
| 11          | R  | 3.58        | 4.68        | 5.97        | 7.56        | 5.43        | 5.88        |
|             | G  | 0.00        | 4.25        | 5.65        | 1.62        | 6.15        | 6.15        |
|             | B  | 3.43        | 4.49        | 5.65        | 5.49        | 4.93        | 5.47        |
| 12          | R  | 2.45        | 4.03        | 3.89        | 0.94        | 3.25        | 3.98        |
|             | G  | 0.00        | 4.80        | 5.99        | 4.58        | 5.60        | 5.60        |
|             | B  | 3.62        | 5.35        | 4.45        | 8.40        | 5.64        | 5.76        |
| 13          | R  | 3.40        | 5.62        | 4.16        | 8.01        | 4.66        | 5.33        |
|             | G  | 0.00        | 5.05        | 5.85        | 4.26        | 5.47        | 5.47        |
|             | B  | 3.40        | 5.62        | 4.29        | 6.60        | 4.52        | 5.20        |
| 14          | R  | 3.74        | 5.23        | 6.08        | 6.59        | 4.98        | 5.77        |
|             | G  | 0.00        | 4.98        | 5.55        | 1.20        | 6.02        | 6.02        |
|             | B  | 3.70        | 4.97        | 5.88        | 5.78        | 5.08        | 5.76        |
| 15          | R  | 3.41        | 4.84        | 6.01        | 6.00        | 5.42        | 6.00        |
|             | G  | 0.00        | 4.58        | 5.66        | 0.73        | 5.92        | 5.92        |
|             | B  | 3.21        | 4.39        | 5.32        | 5.25        | 4.60        | 5.17        |
| <b>mean</b> |    | <b>2.31</b> | <b>5.40</b> | <b>5.32</b> | <b>5.36</b> | <b>5.20</b> | <b>5.68</b> |

Table 1. PSNR improvement in dB over bilinear interpolation for various interpolation methods, for the first 15 images in the Kodak set [6] A) Freeman [2],[5]; B) Hamilton-Adams [6],[7]; C) Chang et. al. [8]; D) Kimmel 0; E) Pei-Tam [4]; F) proposed method. Data in columns B–D are from Table III in [6].



**Figure 3.** Demosaicing results for various interpolation algorithms. From left to right; top row: original, bilinear, Freeman [2],[5]; middle row: Laroche-Prescott [2],[6], Hamilton-Adams [6],[7], Chang et. al. [8]; bottom row: Pei-Tam [4], Kimmel [3], and our proposed method.

## 5. CONCLUSION

We presented a new demosaicing method for color interpolation of images captured from a single CCD using a Bayer color filter array. The proposed linear filters are nearly optimal in a Wiener sense, and in fact outperform many more complex nonlinear filters. Compared to a recently introduced linear demosaicing approach [4], our filters produce a 0.5 dB improvement in interpolated image quality (a 12% reduction in mean-square error), which comes from the same quality for the green channel and about 0.7 dB improvement for the R and B channels. Compared to [4], our method also leads to a small reduction (roughly 12%) in computational complexity.

## REFERENCES

- [1] P. Longère, X. Zhang, P. B. Delahunt, and D. H. Brainard, "Perceptual assessment of demosaicing algorithm performance," *Proc. IEEE*, vol. 90, pp. 123–132, Jan. 2002.
- [2] R. Ramanath, W. E. Snyder, and G. L. Bilbro, "Demosaicking methods for Bayer color arrays," *J. Electronic Imaging*, vol. 11, pp. 306–315, July 2002.
- [3] R. Kimmel, "Demosaicing: image reconstruction from color CCD samples," *IEEE Trans. on Image Processing*, vol. 8, pp. 1221–1228, Sept. 1999.
- [4] S.-C. Pei and I.-K. Tam, "Effective color interpolation in CCD color filter array using signal correlation," *Proc. ICIP*, pp. 488–491, Sept. 2000.
- [5] D. R. Cok, "Reconstruction of CCD images using template matching," *Proc IS&T Annual Conf. / ICPS*, pp. 380–385, 1994.
- [6] B. K. Gunturk, Y. Altunbasak, and R. M. Mersereau, "Color plane interpolation using alternating projections", *IEEE Trans. on Image Processing*, vol. 11, pp. 997–1013, Sept. 2002.
- [7] J. E. Adams, Jr., "Design of practical color filter array interpolation algorithms for digital cameras," *Proc. SPIE*, vol. 3028, pp. 117–125, Feb. 1997.
- [8] E. Chang, S. Cheung, and D. Y. Pan, "Color filter array recovery using a threshold-based variable number of gradients," *Proc. SPIE*, vol. 3650, pp. 36–43, Jan. 1999.
- [9] X. Wu and N. Zhang, "Primary-consistent soft-decision color demosaic for digital cameras," *Proc. ICIP*, vol. I, pp. 477–480, Sept. 2003.